

## Simultaneous OH and HCHO Laser Induced Fluorescence on Premixed Flames of Various Hydrocarbons

Micheline Auge<sup>1</sup>, Deanna A. Lacoste<sup>2</sup>, François Lacas<sup>3</sup>, Juan-Carlos Rolon<sup>4</sup>

1: Gaz de France, St Denis, France, micheline.auge@gazdefrance.com

2: Laboratory EM2C, Chatenay-Malabry, France, deanna.lacoste@em2c.ecp.fr

3: Laboratory EM2C, Chatenay-Malabry, France

4: Laboratory EM2C, Chatenay-Malabry, France, juan\_carlos.rolon@em2c.ecp.fr

---

**Abstract** During the past decades, an important amount of experimental works has been dedicated to the detection of the local Heat Release Rate (HRR) which is of great interest in understanding the behaviour of turbulent flames, in particular in IC engines. Previous studies have shown that convolution of Laser Induced Fluorescence signals of hydroxyl radical (OH) and formaldehyde (HCHO) under atmospheric conditions was a promising way to estimate the heat release rate Najm et al. (1998), Paul and Najm (1998), Fayoux et al. (2004), Böckle et al. (2000). In this study, we investigate the performance of simultaneous LIF measurements of OH and HCHO for laminar stoichiometric premixed methane, n-heptane and isooctane counter-flow flames from 1 to 5 bar.

Experiments were carried out in an axi-symmetrical premixed counter-flow burner producing two planar flames stabilized around the stagnation plane, Rolon et al. (1991), Lacas et al. (1992). The flames are excited by two vertical coplanar laser sheets crossing the burner's axis. The first laser sheet is generated by a frequency-doubled Nd:YAG laser at 532 nm pumping a Dye laser, which frequency is also doubled. This first laser sheet is used in order to excite the OH radical in the  $A^2S - X^2P (1-0) Q_1(6)$  band at 282.93nm (25 mJ, 7 ns pulse duration). The second laser sheet is generated by a Nd:YAG laser frequency tripled at 355 nm (50mJ, 7ns pulse duration) in order to excite HCHO in the  $A^1A_2 - X^1A_1 4^1_0$  band. The two laser beams are synchronized and expanded by cylindrical and spherical lenses to form two coplanar sheets. The LIF signals are collected by two Intensified CCD cameras equipped with two different interferential filters (305-390 nm for OH and 385-450 nm for HCHO).

OH and HCHO profiles across the flames are measured from the LIF images and are multiplied to obtain the local HRR for all hydrocarbon fuels and pressures between 1 and 5 bar. The HRR profiles have also been used to determine the laminar flame speed by computed the distance between the two flames fronts. We could also estimate the flame thickness that corresponds to the half width distance of the HRR peak.

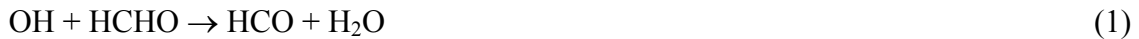
---

### 1. Introduction

During the past decades, an important amount of experimental works has been dedicated to the detection of the reaction zone, the determination of the local heat release rate being of great interest in understanding the behavior of turbulent flames, in particular in IC engines. The aim of this study is to evaluate performances of an optical diagnostic technique based on simultaneous Laser Induced Fluorescence (LIF) of hydroxyl radical (OH) and formaldehyde (HCHO), in order to estimate the heat release rate and to measure overall quantities such as flame speed and flame thickness. As a consequence, such a technique would be of great help for kinetic schemes validation.

Previous studies have shown that a convolution of LIF signals of OH and HCHO under atmospheric conditions was a promising way to estimate the heat release rate. To estimate experimentally such a rate, Najm et al. (1998) have shown the existence of a spatial and temporal correlation between formyl radical (HCO) concentration and heat release rate. When applied to a laminar premixed flame under atmospheric pressure, the HCO fluorescence signal was unfortunately not sufficient to provide accurate signal-to-noise ratio. Considering this technique as a single-pulse imaging diagnostic in turbulent combustion seems therefore not yet available. However, in the meantime,

Paul et al. (1998) have established the correlation between HCO production and the concentration of OH and HCHO with the reaction:



As OH and HCHO species appear in relatively large quantities in the reaction zone, this technique allows a measurement of the heat release rate (HRR) in different turbulent environments, Fayoux et al. (2004), Böckle et al. (2000). The results obtained have shown a good agreement between experimental and numerical comparisons thus validating this measuring technique for atmospheric methane air flames.

However, before applying this method in realistic IC engines, it is necessary to study the influence of pressure and fuel on the LIF signals of OH and HCHO and their product, and to compare the results. We investigate here the performance of simultaneous LIF measurements of OH and HCHO for laminar stoichiometric premixed methane, n-heptane and isooctane counter-flow flames from 1 to 5 bar. After describing the experimental setup, the feasibility of simultaneous fluorescence imaging of OH and HCHO in flames under pressure is demonstrated. The heat release rate profiles have been computed and also used to determine the laminar flame speed by computed the distance between the two flames fronts, and the flame thickness, which corresponds to the half width distance of the HRR peak. A comparison with analytical results demonstrates the good accuracy of this technique.

## 2. Experimental setup

Experiments were carried out in an axi-symmetric premixed counterflow burner producing two planar flame fronts stabilized around the stagnation plane, Rolon et al. (1991), Lacas et al. (1992). As shown on Fig. 1, the burner consists of two opposed axi-symmetric 10 mm diameter injection nozzles. The distance between the two nozzle exits is  $d=10\text{mm}$ . Air and gaseous fuel are first mixed together in a cylindrical mixing chamber (80 mm diameter and 200 mm long). The premixed gas flow issuing the premixed chamber is then divided in two flows feeding the two parts of the burner providing the same velocity on both sides (1 m/s). The two flows are equilibrated with a balance valve. In both upper and lower burners, an annular flow of nitrogen is injected through a coaxial nozzle in order to insulate the inner premixed flow from external perturbations and surrounding atmosphere.

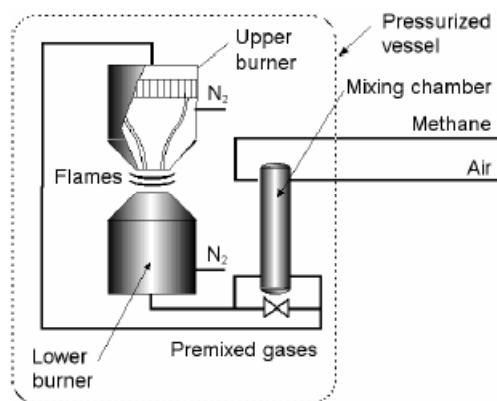


**Fig. 1** Schematic view of the burner

A vaporization system was used for n-heptane and isooctane, as shown in Fig. 2. A tank filled with the liquid fuel is placed under the pressure chamber. A flow of air enters the tank by a tube placed

at the bottom. The part of the tube in the tank is perforated by twenty-five 1 mm diameter holes to allow the air to bubble in the liquid fuel. The tank of fuel is placed in a warm bath of water. The temperature of the bath is controlled to have a saturated vapor pressure of liquid fuel high enough to charge the bubbles of air in fuel. Then the air is conducted to the premixed chamber where additional air is added to have the right fuel/air ratio with the different pressures used.

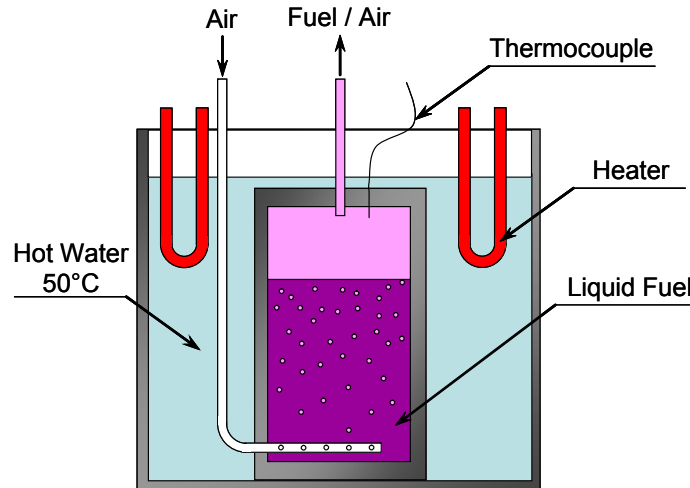


Fig. 2 Schematic view of the vaporization system

The burners and the mixing chamber are placed in a 40 l high-pressure vessel, which maintains a uniform pressure in the whole experimental area. The high-pressure vessel is equipped with four large quartz windows (40 mm in diameter), as shown in Fig. 3. A set of mass flow meters (*Bronkhorst Elflow*) controls the air, fuels and nitrogen flow rates. The pressure in the vessel is controlled with a sonic nozzle and pressure may be adjusted from 1 to 30 bar. A complete description of the experimental setup may be found in Böhm and Lacas (2000).

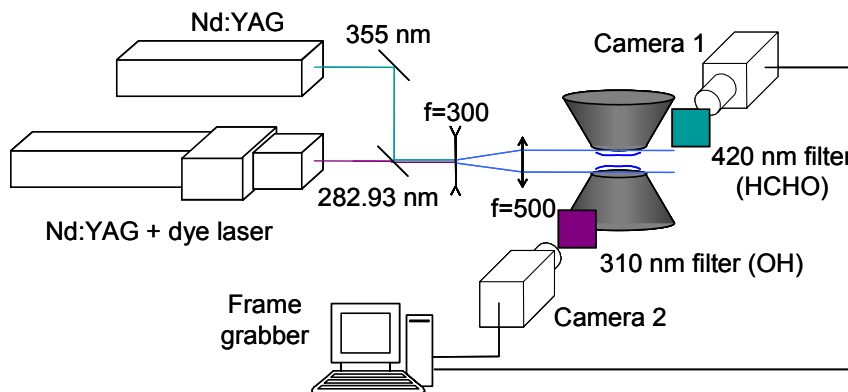


Fig. 3 Schematic view of the optical mount

### 3. Optical diagnostics

The flames generated in the counterflow burner are excited by two vertical coplanar laser sheets crossing the burner's axis, as shown on Fig. 3. A laser sheet generated by a frequency-doubled Nd:YAG laser to pump a Dye laser (Rhodamine 590), which frequency is doubled, is used in order to excite the OH radical in the  $A^2\Sigma - X^2\Pi$  (1-0)  $Q_1(6)$  band at 282.93 nm (25 mJ, 7ns pulse duration). The laser beam issued from the Dye laser is expanded through cylindrical and spherical

UV lenses ( $f_{\text{cyl}} = 300 \text{ mm}$ ,  $f_{\text{sph}} = 500 \text{ mm}$ ) to form a  $15 \text{ mm} \times 0.5 \text{ mm}$  sheet. An Intensified CCD camera (*Princeton Instruments*,  $512 \times 512$  pixels, 16 bit) is placed perpendicular to the axis of the laser sheet to detect the fluorescence signal issued from the excitation of OH. The camera is equipped with a  $105 \text{ mm f/4.5 UV-Nikkor}$  lens. The collection of the OH fluorescence is realized between 305 and 390 nm within the  $A^2\Sigma-X^2\Pi$  (1-1) and (0-0) band with two filters referenced UG5 ( $320 \text{ nm FWHM}=150\text{nm}$  band pass filter) and WG305 ( $305 \text{ nm}$  low pass filter), as shown in Fig. 3. The second laser sheet is generated by a Nd:YAG laser frequency tripled at  $355 \text{ nm}$  ( $50 \text{ mJ}$ ,  $7 \text{ ns}$  pulse duration) in order to excite HCHO in the  $A^1A_2 - X^1A_1 4^1_0$  band. The laser beam issued from Nd:YAG laser is expanded through the same lenses as for the OH excitation laser. Detection of HCHO fluorescence signal is performed using a second Intensified CCD camera (*Princeton Instruments*,  $512 \times 512$  pixels, 16 bit). The camera is equipped with a  $105 \text{ mm f/4.5 UV-Nikkor}$  lens. The collection of the HCHO fluorescence is realized between 385 and  $490 \text{ nm}$  with a combination of a  $385 \text{ nm}$  high-pass (GG385) and  $450 \text{ nm}$  low-pass (03SWP606) filters as shown in Fig. 3. The two laser beams form two coplanar sheets with the same dimensions ( $0.5 \times 15 \text{ mm}$ ). The two detection cameras are synchronized and are set to observe images of the same size, to enable images comparison. In order to identify the fluorescence signals, one of the cameras could be replaced by a spectrometer (Acton Research SP300i, grating 600 BLZ  $500 \text{ nm}$ ). The spectrometer's detector is an ICCD camera (*Princeton Instruments*  $512 \times 512$  pixels, 16bit) and it is calibrated with a Hg lamp. Two spherical lenses ( $f_{\text{sph}} = 150$  and  $500 \text{ mm}$ ) collect the fluorescence signal issued from the flames and collimate it on the spectrometer's slit. The same set of filters used for OH or HCHO PLIF imaging is placed in front of the entrance slit of the spectrometer in order to eliminate the excitation wavelength. The spectra were recorded for the different pressures, as shown in Fig. 4, and compared with the available literature to confirm the presence of OH and HCHO, Harrington and Smith (1993), Herzberg (1988).

#### 4. Experimental results

In this work premixed stoichiometric methane/air, n-heptane/air and isooctane/air flames are studied. The fresh mixture is injected in the two parts of the burner at  $1 \text{ m/s}$ . The flow meters are used to keep the mixture velocity and the fuel/air ratio constant with pressure changes. In this condition we estimate the strain rate of the flame at  $220 \text{ s}^{-1}$ . Spectroscopic measurements were performed to validate the collected LIF signals. The results obtained for methane/air flames are presented in Fig. 4. The spectral bands observed correspond to OH and HCHO fluorescence bands, Harrington and Smith (1993), Herzberg (1988), and their intensities are decreasing strongly with pressure, probably due to an increase of quenching. Equivalent results have been obtained for both others fuels.

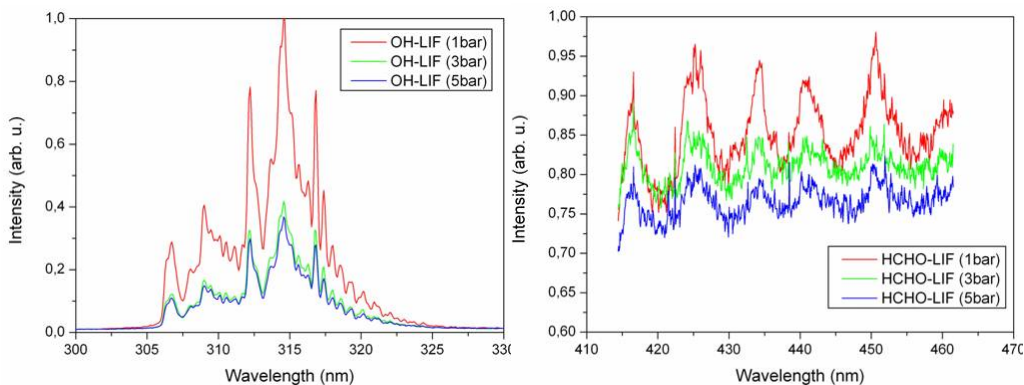


**Fig. 4** OH (left) and HCHO (right) LIF spectra for 1, 3 and 5 bar

Both cameras images have the same size, their superposition leads to an error of  $\pm 1$  pixel (= 0.1 mm). 100 images are recorded for each measurement but the analysis of the profiles was done on individual images. The flames are not perfectly flat thus it is not possible to extract one single representative vertical profile on the flame axis. 8 squares of 15 pixels large are thus selected near the jet axis. Eight vertical profiles are extracted from the squares by summing the intensities of the 15 pixels in width. This size allows a good compromise between signal to noise ratio and flame thickness.

The simultaneous OH and HCHO LIF images obtained for methane/air, n-heptane/air and isooctane/air flames are presented respectively in Fig. 5, 6 and 7 with the associated color scale. The signal to noise ratio is larger for OH than for HCHO fluorescence. The images show that HCHO exists in a thin region near the flame front in the fresh gases. Conversely OH is present in a large region in the burnt gases. For pressures up to 3 bar, large convective instabilities are visible in the extremities of the flames, probably due to the difference of density between the burnt high temperature gases and the cold surrounding nitrogen.

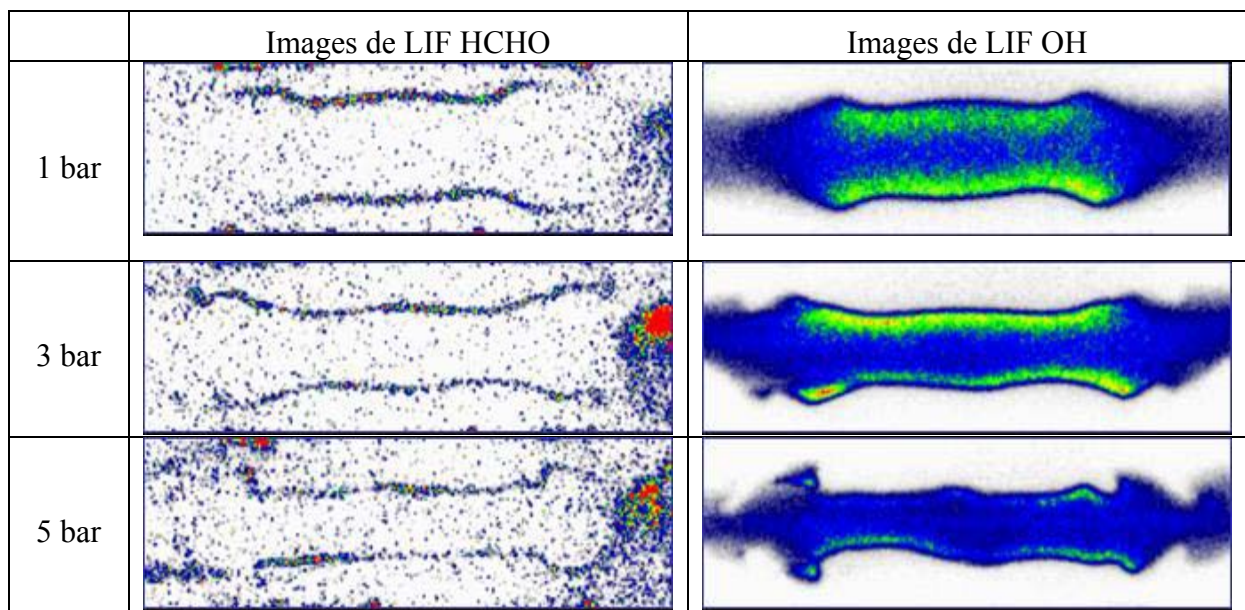


**Fig. 5** OH and HCHO LIF images obtained for stoichiometric methane/air premixed flames

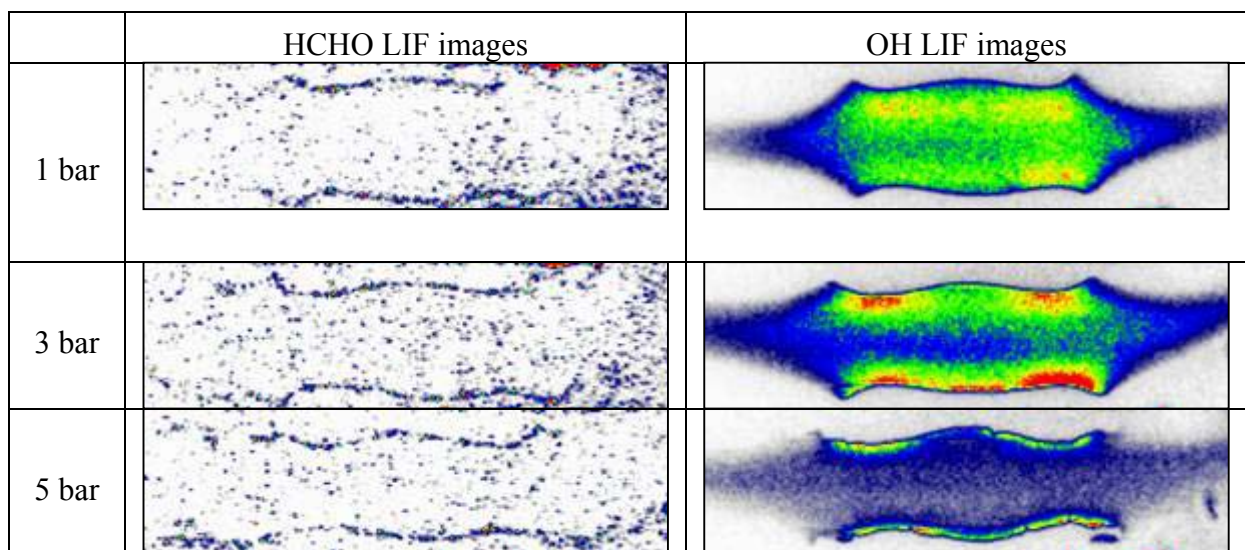


**Fig. 6** OH and HCHO LIF images obtained for stoichiometric n-heptane/air premixed flames

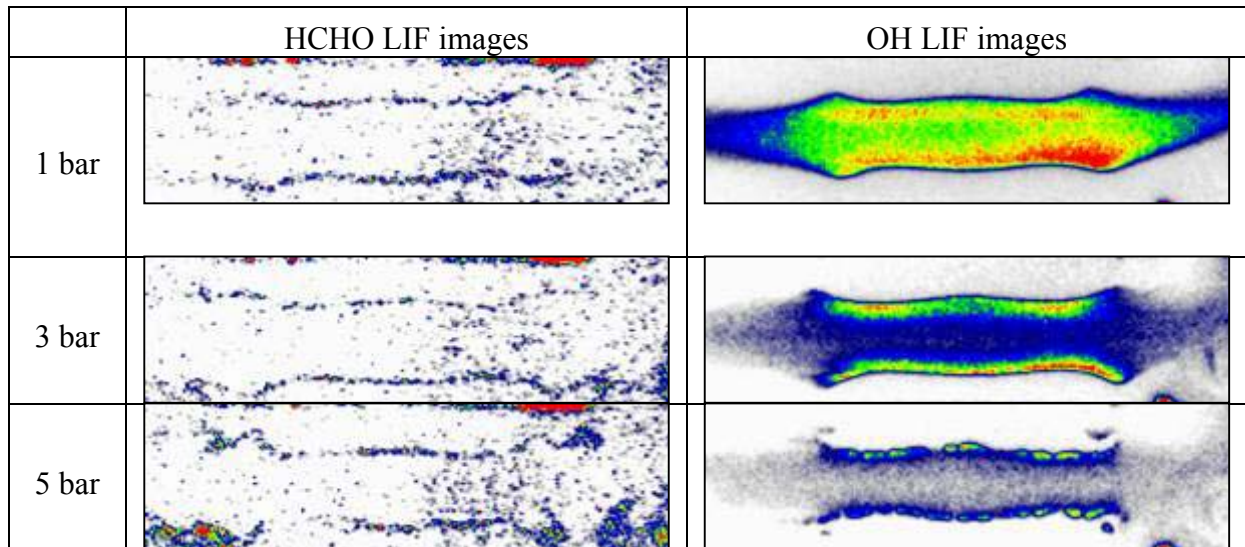
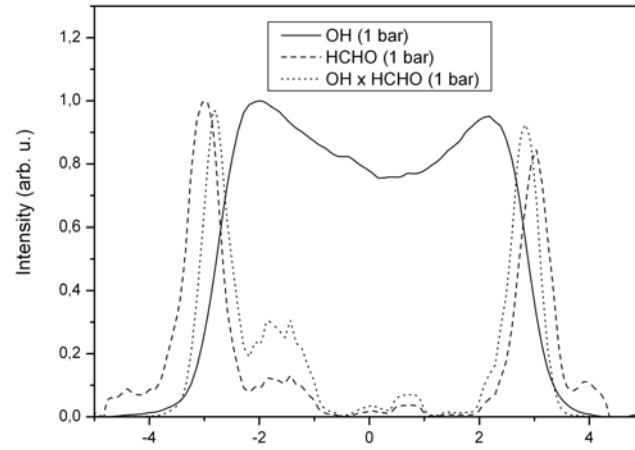
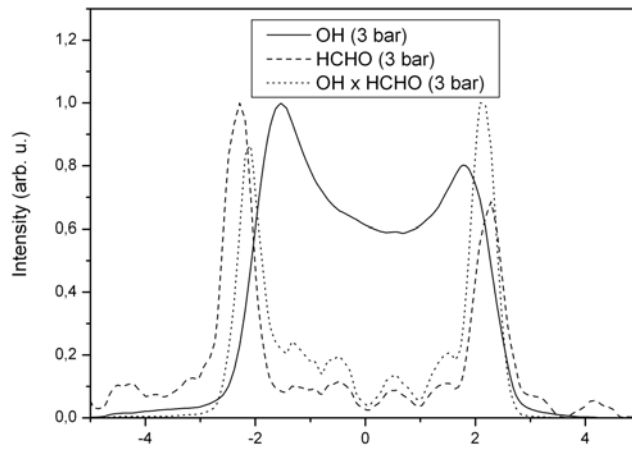


**Fig. 7** OH and HCHO LIF images obtained for stoichiometric isooctane/air premixed flames

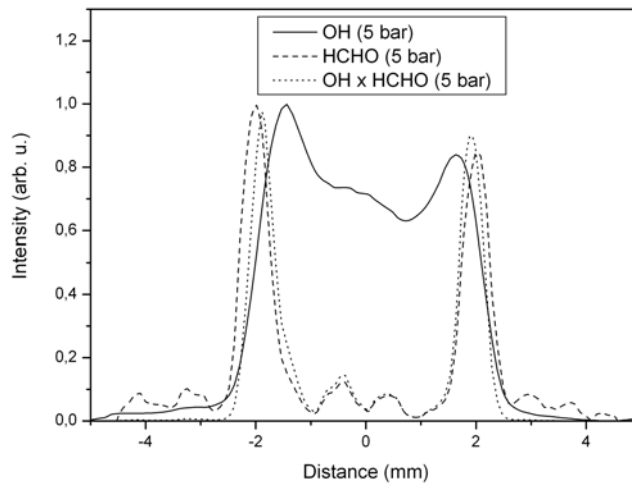
For all fuels, OH and HCHO LIF profiles are extracted from the fluorescence images and are multiplied to obtain local heat release rate (HRR), as presented in Fig. 8, 9 and 10. From the HRR profiles we have computed the distance between the two flames fronts corresponding to the distance between the two peaks. We have also estimated the flame thickness that corresponds to the half width distance of the HRR peak. This has been done for the 8 boxes of 100 individual images. We can thus obtain a mean distance and mean flame thickness by averaging the 800 values. We observed that, when increasing the pressure, the distance between the two flames decreases.



(a)



(b)



(c)

**Fig. 8** OH, HCHO and OHxHCHO LIF profiles obtained for stoichiometric methane/air premixed flames (a) 1 bar, (b) 3 bar and (c) 5 bar

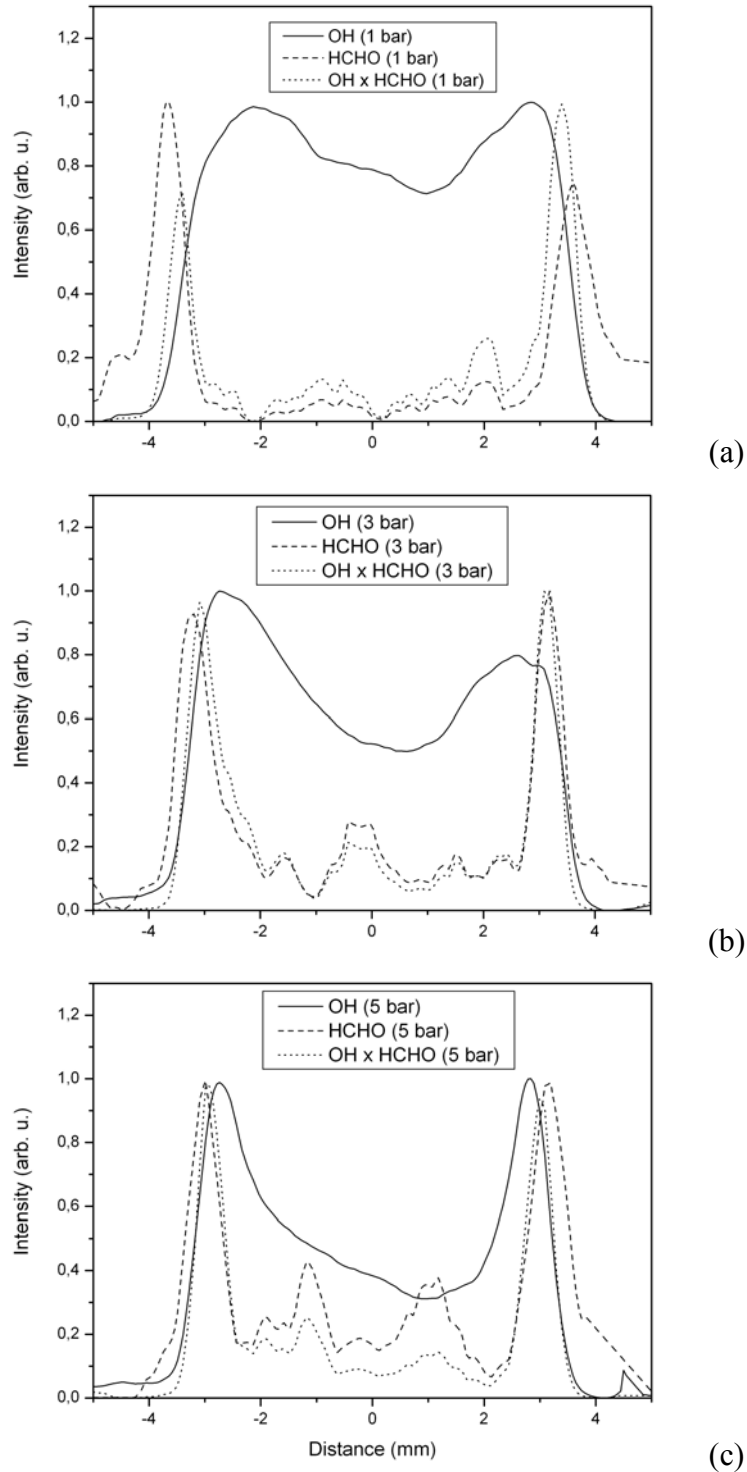
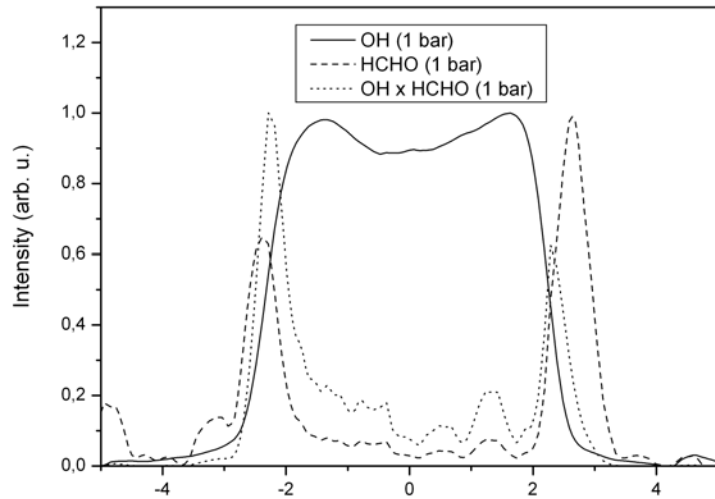
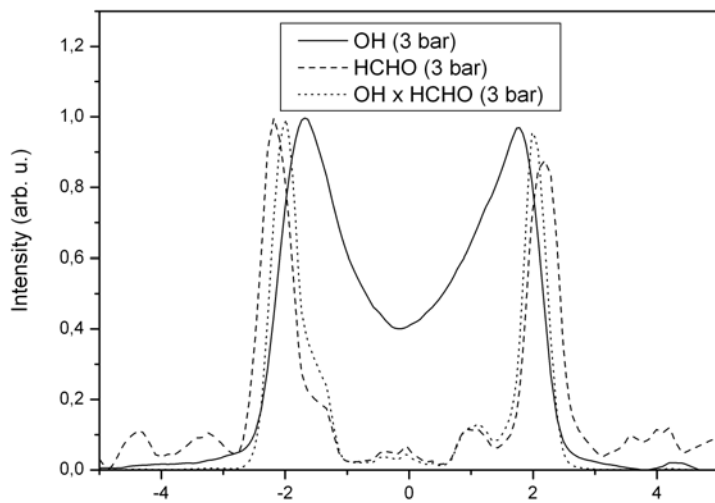


**Fig. 9** OH, HCHO and OHxHCHO LIF profiles obtained for stoichiometric n-heptane/air premixed flames (a) 1 bar, (b) 3 bar and (c) 5 bar

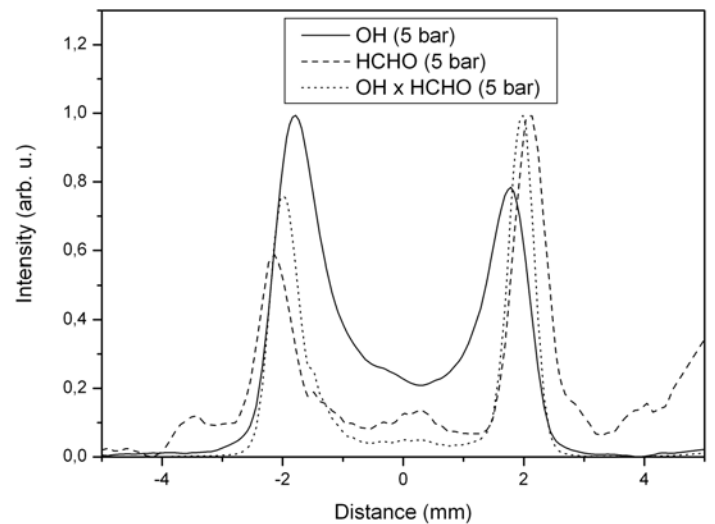




(a)



(b)



(c)

**Fig. 10** OH, HCHO and OHxHCHO LIF profiles obtained for stoichiometric isoctane/air premixed flames (a) 1 bar, (b) 3 bar and (c) 5 bar

## 5. Discussion

Flame characteristics, such as laminar flame speed or thickness, may be deduced from the knowledge of HRR profile. The HRR profiles allow us to determine the distance between the two flames. This distance has been calculated for each of the 100 images recorded for the 3 pressures studied. As mentioned before, for each image, 8 profiles have been determined and thus 8 values of the distance between the two flames. We obtain thus an average value of the distance between the two flames and the associated fluctuations, represented as error bars on the plots. The knowledge of this distance allows us to determine the experimental laminar flame speed  $S_{Lexp}$ . The laminar flame front is always located at a point where the local gas velocity is equal to the laminar flame speed. But as no experimental velocity measurements are available in our high pressure configuration, a rough estimate may be done by assuming a linear decrease of the velocity between the injector exit and the stagnation point located at the half distance between the two flame fronts, Rolon et al. (1991). Therefore we can estimate the laminar flame speed  $S_{Lexp}$  as:

$$S_{Lexp} = d_{if} * V_{inj} / d \quad (2)$$

where  $V_{inj}$  is the velocity of the injected flow,  $d_{if}$  is the average distance between the two flames and  $d$  is the distance between the two burners. In fact in a strained counterflow flame the gas velocity decreases in the fresh gases and at the flame front the velocity increases very rapidly. The gas velocity at the flame front is then equal to the flame speed. The experimental flame speeds are plotted on Fig. 11 and the results obtained for methane/air flames are compared to the results that may be obtained by using the analytical formulation proposed by Poinso and Veynante (2005), noted  $S_{LPoinso}$ . For this fuel, under atmospheric pressure, analytical and experimental techniques provide the same values. We observe a difference of 20 % at 3 and 5 bar between the experimental  $S_{Lexp}$  and analytical values  $S_{LPoinso}$ . We can conclude that our technique enables an estimation of the order of magnitude of laminar flame speed.

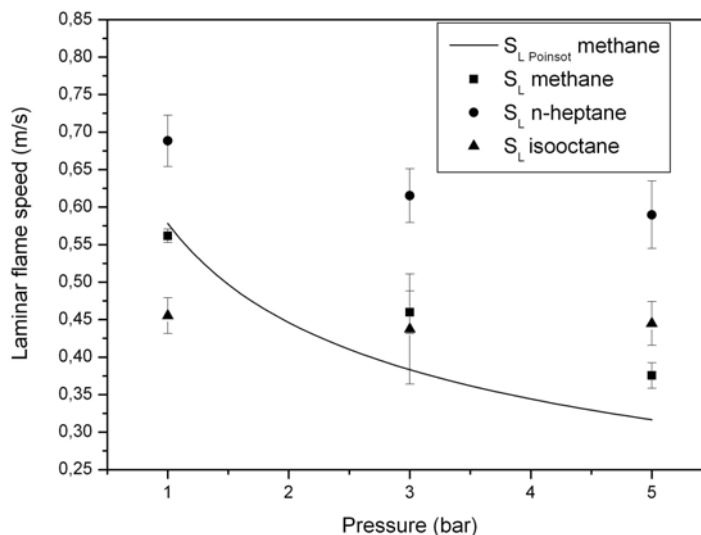


**Fig. 11** Experimental and analytical laminar flame speed as a function of pressure

The flame thickness may also be computed from HRR by taking the value of the thickness of the HRR peak at mid height of the tip. This was extracted for all the images (800 for each pressure) and, for methane/air flames, we then compared to analytical thickness, Poinso and Veynante (2005). Analytical and experimental flame thicknesses have been plotted as a function of pressure on Fig. 12. We observe a great discrepancy in the results depending on the method used.. The

general trend of analytical results is that flame thickness decreases when pressure rises. For 1 bar, the analytical and experimental results show relatively good agreement. The difference is less than 10 %. But for 3 and 5 bar, the analytical results show a decrease in the value of the flame thickness when pressure rises conversely to experimental results. The difference is then 45 % for 3 bar and 65 % for 5 bar. This could be explained by a very low signal-to-noise ratio for pressures over 1 bar as we can show on Fig. 5, 6 and 7.

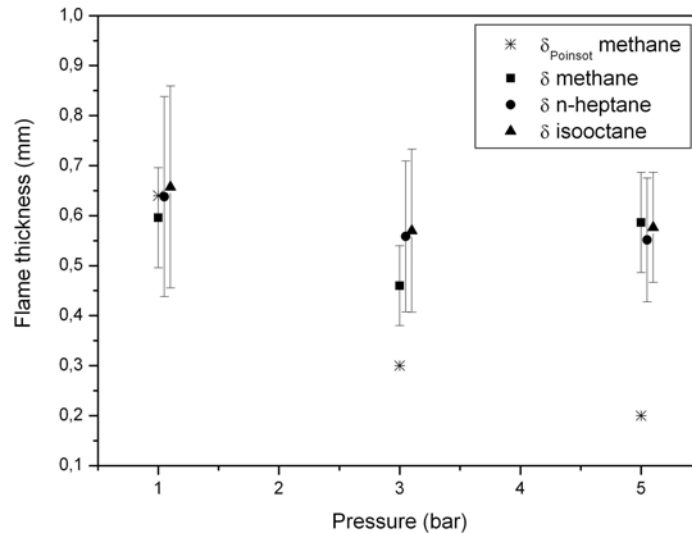


Fig. 12 Experimental and analytical flame thickness as a function of pressure

## 6. Conclusions

We have shown that simultaneous LIF imaging of OH and HCHO species under pressure (1, 3 and 5 bar) is possible for stoichiometric premixed methane/air, n-heptane/air and isooctane/air flames and then, a good estimation of the HRR is possible. This method is of great interest for IC engines local heat release rate measurements. In fact up to now in these engines only global heat release rate has been measured. The measured HRR profiles have been analyzed to determine quantitative values of flame thickness and laminar flame speed. The experimental results have been compared to analytical values. The experimental results are in good agreement with analytical results in terms of laminar flame speed but underestimate the flame thickness especially at high pressure. The quality of experimental results may be improved by increasing the signal-to-noise ratio of HCHO fluorescence and the spatial resolution of the images. The first point could be achieved by increasing the energy concentration of the laser sheet, e.g. in reducing the height of the laser sheet. The second point implies to change the collecting optics, which is made complex due the limited optical access in the pressurized vessel. Nevertheless, simultaneous fluorescence of OH and HCHO seems to be a promising tool in the context of IC engines.

## Acknowledgements

We would like to express all our thanks to Institut Français du Pétrole for the funding of Miss Micheline Augé PhD studies and the PREDIT program for the grant of Dr Deanna A. Lacoste.

## References

S. Böckle, J. Kazenwadel, T. Kunselmann, D. Shin, C. Schultz, J. Wolfrum, *Proc. Combust. Inst.* 28 (2000) 279-286.

- H. Böhm, F. Lacas, *Proc. Combust. Inst.* 28 (2000) 2627-2634.  
A. Fayoux, K. Zähringer, O. Gicquel, J.C. Rolon, *Proc. Combust. Inst.* 30 (2004) 251-257.  
J.E. Harrington, K.C. Smith, *Chem. Phys. Lett.* 202 (34) (1993) 196-202.  
G. Herzberg, *Molecular spectra and molecular structure Vol. III*, Krieger publishing company, Florida, 1988  
F. Lacas, N. Darabiha, P. Versaevel, J.C. Rolon, S. Candel, *Proc. Combust. Inst.* 24 (1992) 1523-1529  
H. Najm, P. Paul, C. Mueller, P. Wyckoff, *Combust. Flame* 113 (1998) 312-332.  
P. Paul, H. Najm, *Proc. Combust. Inst.* 27 (1998) 43-50.  
T. Poinso, D. Veynante, *Theoretical and numerical combustion*, 2<sup>nd</sup> Edition, Edwards, USA Philadelphia, 2005.  
J.C. Rolon, D. Veynante, J.P. Martin, *Experiments in fluids.* 11 (1991) 313-324.